Journal of Alloys and Compounds 509 (2011) 4774–4780

Contents lists available at ScienceDirect

Journal of Alloys and Compounds

journal homepage: www.elsevier.com/locate/jallcom

Single step synthesis of $GdAlO_3$ powder

Amit Sinha*, S.R. Nair, P.K. Sinha

Energy Conversion Materials Section, Materials Group, Bhabha Atomic Research Centre, Vashi Complex, Navi Mumbai 400705, India

ARTICLE INFO

Article history:
Received 24 September 2010
Received in revised form 18 January 2011
Accepted 20 January 2011
Available online 2 February 2011

Keywords:
Gadolinium aluminate
$GdAlO_3$
XRD
Sintering
Urea
Glycine
β-Alanine
Rietveld analysis

ABSTRACT

A novel method for preparation of nano-crystalline gadolinium aluminate ($GdAlO_3$) powder, based on combustion synthesis, is reported. It was observed that aluminium nitrate and gadolinium nitrate exhibit different combustion characteristics with respect to urea, glycine and β-alanine. While urea was proven to be a suitable fuel for direct formation of crystalline α-Al_2O_3 from its nitrate, glycine and β-alanine are suitable fuels for gadolinium nitrate for preparation of its oxide after combustion reaction. Based on the observed chemical characteristics of gadolinium and aluminium nitrates with respect to above mentioned fuels for the combustion reaction, the fuel mixture composition could be predicted that could lead to phase pure perovskite $GdAlO_3$ directly after the combustion reaction without any subsequent calcination step. The use of single fuel, on the other hand, leads to formation of amorphous precursor powders that call for subsequent calcination for the formation of crystalline $GdAlO_3$. The powders produced directly after combustion reactions using fuel mixtures were found to be highly sinterable. The sintering of the powders at 1550 °C for 4 h resulted in $GdAlO_3$ with sintered density of more than 95%. T.D.

1. Introduction

Gadolinium aluminate ($GdAlO_3$) is a technologically important rare earth based perovskite oxide which finds applications as phosphor [1,2], scintillator [3,4], as well as a potential host system for materials with oxygen ion conductivity [5,6]. Conventionally, $GdAlO_3$ is produced by solid state reaction of gadolina and alumina powders which essentially involves extensive mechanical mixing followed by lengthy heat treatments and sintering at relatively high temperatures (1650–1700 °C) [7]. To circumvent the problems associated with solid state synthesis of $GdAlO_3$ powder, several wet-chemical techniques, such as the polymerized complex route, combustion synthesis, sol–gel have been utilized to synthesize gadolinium aluminate ($GdAlO_3$) [1,2,8–11]. In our previous investigations, $GdAlO_3$ powder was prepared through citrate-nitrate route where citric acid and metal nitrates formed soluble complexes in aqueous solution, which on dehydration yielded an amorphous solid precursor that gave rise to the desired phase only after calcination at 1000 °C for 2 h [5,11]. However, the powder produced through citrate gel route could be sintered to a density greater than 95% T.D. only at 1600 °C [5]. The motivation of the present work was to prepare highly sinterable $GdAlO_3$ powder through combustion synthesis in a single step process.

Combustion synthesis is one of the important processing techniques for synthesis of advanced ceramic powders, where the exothermicity of the redox chemical reaction is utilized to produce powders with desired phase and morphology. This process is characterized by high-temperatures, fast heating rates with rapid reaction times; these features are attractive for the production of technologically important materials as compared to the conventional ceramic processing methods. Combustion synthesis essentially involves a self-sustained reaction in homogeneous solution of different oxidizers (e.g., metal nitrates) and fuels (e.g., urea, glycine, alanine). Several nanocrystalline oxide ceramic powders have recently been successfully prepared through combustion synthesis processes [12–15]. However, similar to the conventional solid state synthesis method, the powders resulting from the traditional combustion synthesis routes, involving the use of a single fuel require additional thermal treatments in order to complete the formation of the desired crystalline phase. The additional calcination step could be removed by judicial selection of fuel–nitrate mixtures. High flame temperature of the combustion reaction, though lasting for a few seconds, is sufficient to form the desired phase from the dried gel. In the present investigation, a systematic study has been carried out to synthesize $GdAlO_3$ using one step solution combustion route that yields the phase pure powder directly after combustion reaction.

2. Experimental

$Gd(NO_3)_3$. $9H_2O$ (99.99% purity, Indian Rare Earth, India), $Al(NO_3)_3{\cdot}9H_2O$ (AR Grade, E-merck India) were used as starting materials. The nitrate solutions were

---

* Corresponding author. Tel.: +91 22 27887161; fax: +91 22 27840032.
E-mail address: amit97@yahoo.com (A. Sinha).

0925-8388/$ – see front matter © 2011 Elsevier B.V. All rights reserved.
doi:10.1016/j.jallcom.2011.01.156

Table 1
Combustion behavior of stoichiometric mixtures of Gd/Al nitrate and three different fuels.

Sr. No.	Sample code	Metal nitrate(s)	Fuel(s)	Combustion reaction	Phase analysis by XRD	Remarks
1	Gd-U	$Gd(NO_3)_3$	Urea	No Combustion	Amorphous	White colored powder
2	Gd-G		Glycine	Flame combustion	m-Gd_2O_3	Phase formation after combustion
3	Gd- B		β-Alanine	Violent flame combustion	m-Gd_2O_3	Phase formation after combustion
4	Al-U		Urea	Flame combustion	α-Al_2O_3	Phase formation after combustion
5	Al-G	$Al(NO_3)_3$	Glycine	Sluggish Combustion	Amorphous	Brown colored powder
6	Al-B		β-Alanine	Sluggish Combustion	Amorphous	Brown colored powder
7	GA-U		Urea	No combustion	Amorphous	White colored powder
8	GA-G	$Gd(NO_3)_3$+ $Al(NO_3)_3$	Glycine	Sluggish Combustion	Amorphous	Brown colored powder
9	GA- B		β-Alanine	Sluggish Combustion	Amorphous	Brown colored powder
10	GA-UG	$Gd(NO_3)_3$+ $Al(NO_3)_3$	Urea + glycine	Flame combustion	$GdAlO_3$	Phase formation after combustion
11	GA-UB		Urea + β-alanine	Flame combustion	$GdAlO_3$	Phase formation after combustion

analyzed for metal ion concentration. The metal ions were complexed by stoichiometric quantities of a fuel or fuel mixture. The composition of fuel and metal nitrates were calculated based on the method of Jain et al. [16] where a 'stoichiometric' composition denotes a fuel-to-nitrate ratio in which the fuel reacts completely with all of the metal nitrates.

In the present investigation, three different fuels, e.g., urea (CH_4N_2O), glycine ($C_2H_5NO_2$) and β-alanine ($C_3H_7NO_2$) (all AR Grade), were utilized. The fuels used in combustion synthesis serve two purposes. Firstly, they form complexes with the metal ions facilitating molecular level mixing of cations in solution. Secondly, they act as a source of carbon and hydrogen, which on combustion, liberate heat. Depending upon the fuels used, the exothermicity of the redox reaction varies and the combustion characteristics of metal ions differ from flaming to non-flaming (smoldering). According to the stoichiometric concept in combustion synthesis [16], the ratio of the net oxidizing valency of the metal nitrate to the net reducing valency of fuel should be unity. Based on the oxidizing valences of oxidants and reducing valences of different fuels used in the present investigation, the molar ratio of fuel to metal nitrates were determined.

In the present process, the mixed solution, of metal nitrates and fuel(s), was slowly dehydrated on a hot plate to form a viscous, transparent gel. Depending on the type of fuel or mixture of fuels used, either gel was transformed into an amorphous precursor powder or a combustion reaction took place that yielded powder with desired phase. The flame temperatures of the combustion reactions were measured using an optical pyrometer (Minolta/Land Cyclops 52, Minolta Camera Co. Japan/Land Integrated Ltd. England).

Initially, the individual combustion characteristics of $Gd(NO_3)_3$ and $Al(NO_3)_3$ with respect to urea, glycine and β-alanine were investigated. For this purpose, combustion behavior of stoichiometric mixtures of Gd/Al nitrate and three different fuels were studied. Based on the combustion characteristics of individual metal ions, $GdAlO_3$ powder was prepared using a fuel mixture of urea + β-alanine or urea + glycine. For this purpose, equimolar amounts of Gd- and Al- nitrate solutions were mixed with the fuel mixture which on dehydration led to flame combustion yielding a white powder.

The powders obtained after combustion reactions as well as calcined powders were characterized by X-ray diffraction (Philips Analytical, Model PW1710) for phase analysis. Standard silicon sample supplied by the manufacturer was employed as internal standard for calibration. The XRD patterns were recorded at a scan rate of 0.025°/s using CuKα radiation. The average crystallite sizes of the crystalline powders produced in the present investigation were determined from the X-ray line broadening using the Scherrer's formula [17]:

$$D = \frac{0.9\lambda}{\beta \cos\theta} \tag{1}$$

where D is the average crystallite size (Å), λ is the wavelength of X-ray used (1.54 Å), θ is the angle of diffraction, β is full widths (in radian) at half maximum observed for the sample. The lattice parameters of $GdAlO_3$ were determined using Rietveld refinement on XRD data. Rietveld analysis was performed using Fullprof program incorporated in the WinPLOTR software package [18].

The particle size distribution of $GdAlO_3$ powders was measured by laser diffraction particle size analyser (HORIBA LA–500). In order to carry out the sintering study, as-produced $GdAlO_3$ powders, without any further milling, were compacted in a uniaxial hydraulic press at 100 MPa and subsequently sintered in the temperature interval of 1400–1550 °C for 4 h in air. The morphological characterisation of powder particles as well as microstructural analysis of the sintered samples were carried out by scanning electron microscopy (SERON AIS2100). From the SEM images, the grain sizes of the sintered materials were estimated using the linear intersect method, according to the relation

$$\bar{G} = \frac{1.57}{N_L}$$

Here $\bar{G}$ is the mean grain size, N_L is the number of counted grains divided by the length of the test line and the constant 1.57 is a dimensionless correction factor [19] accounting for the arbitrary intercepts of the plane and of the test line with respect to the grains. The relative densities of sintered specimens were measured

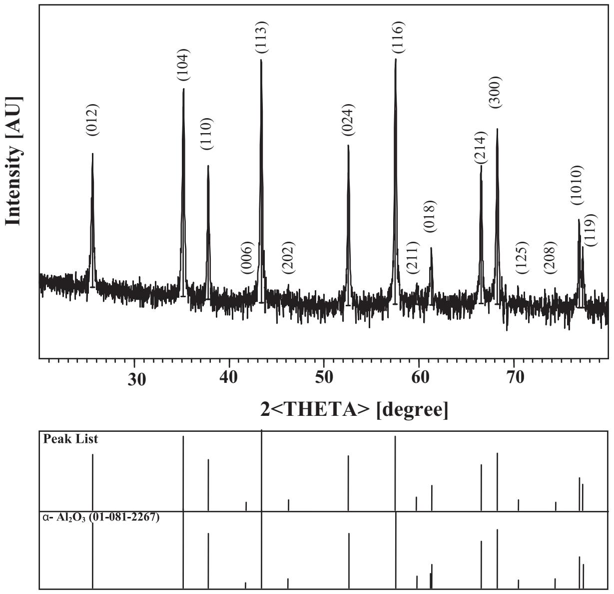

Fig. 1. XRD pattern of alumina powder produced through combustion reaction of aluminium nitrate and urea.

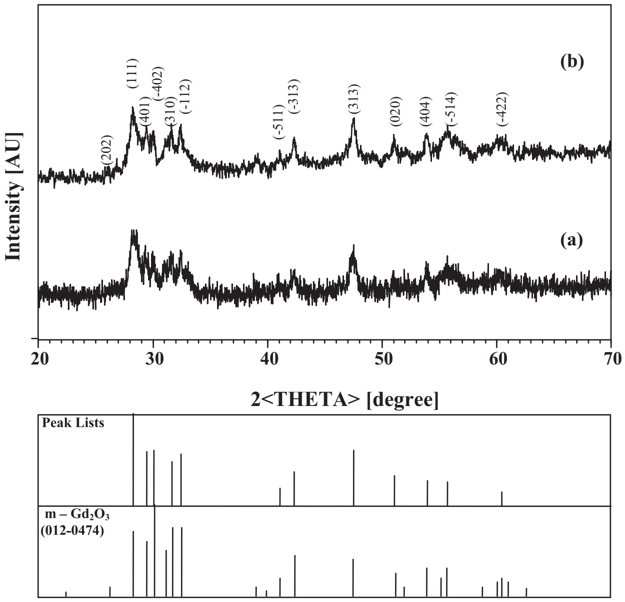

Fig. 2. XRD patterns of Gd_2O_3 powders produced through combustion reactions of gadolinium nitrate with (a) glycine; (b) β-alanine.

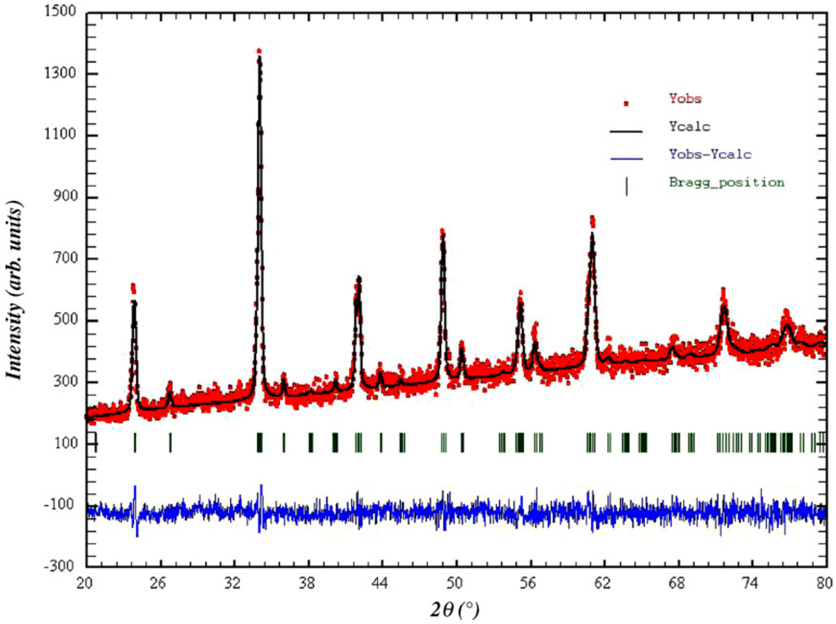

Fig. 3. XRD pattern of $GdAlO_3$ powder produced through combustion reaction of gadolinium–aluminium nitrates with urea and β-alanine. The calculated and observed patterns are shown in the top by the solid line and the dots respectively. The vertical marks in the middle show positions calculated for Bragg reflection. The trace in the bottom is a plot of the difference: observed minus calculated.

using Archimedes water displacement technique, assuming theoretical density of $GdAlO_3$ to be 7.442 kg/m^3 [ICDD PDF 046-0395].

3. Results and discussion

3.1. Preparation of powder

3.1.1. Use of single fuel

The details of the combustion behavior of stoichiometric mixtures of Gd/Al nitrate and three different fuels are shown in Table 1. It was observed that the stoichiometric mixture of aluminium nitrate and urea resulted in a fast combustion reaction yielding a white powder. The XRD pattern of the powder is shown in Fig. 1. All the reflections of the pattern could be indexed to α-Al_2O_3 [ICDD PDF 081-2267]. The average crystallite size of the powder is 31 nm. On the other hand, stoichiometric mixture of $Gd(NO_3)_3$ and urea did not lead to any sort of combustion and resulted in a black powder; the amorphous nature of this powder was confirmed by XRD. The difference between the chemical behavior of $Gd(NO_3)_3$ and $Al(NO_3)_3$ with respect to urea was also observed in the combustion characteristics manifested by the two metal nitrates towards glycine, and β-alanine. The mixtures of $Al(NO_3)_3$–glycine and $Al(NO_3)_3$–β-alanine exhibited only sluggish combustion. The products obtained in both these cases were brown

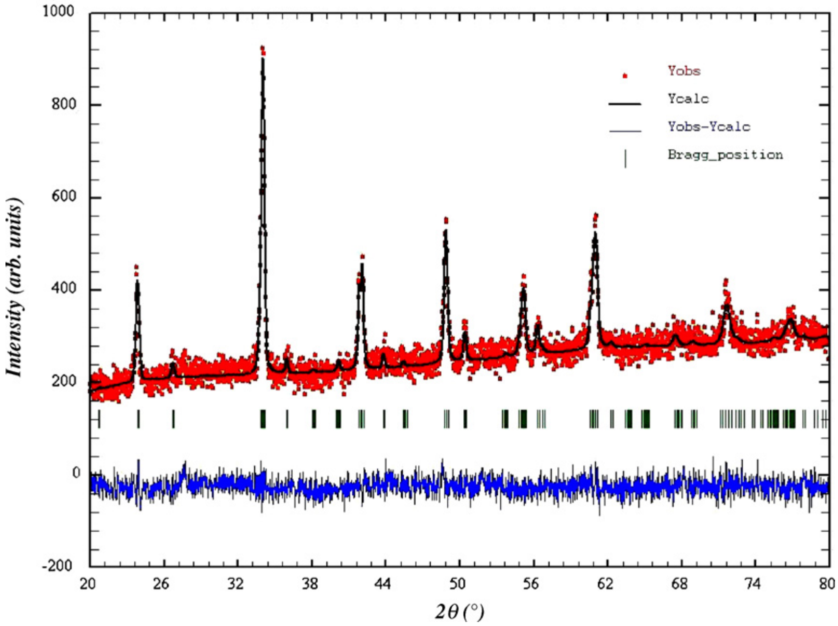

Fig. 4. XRD pattern of $GdAlO_3$ powder produced through combustion reaction of gadolinium–aluminium nitrates with urea and glycine. The calculated and observed patterns are shown in the top by the solid line and the dots respectively. The vertical marks in the middle show positions calculated for Bragg reflection. The trace in the bottom is a plot of the difference: observed minus calculated.

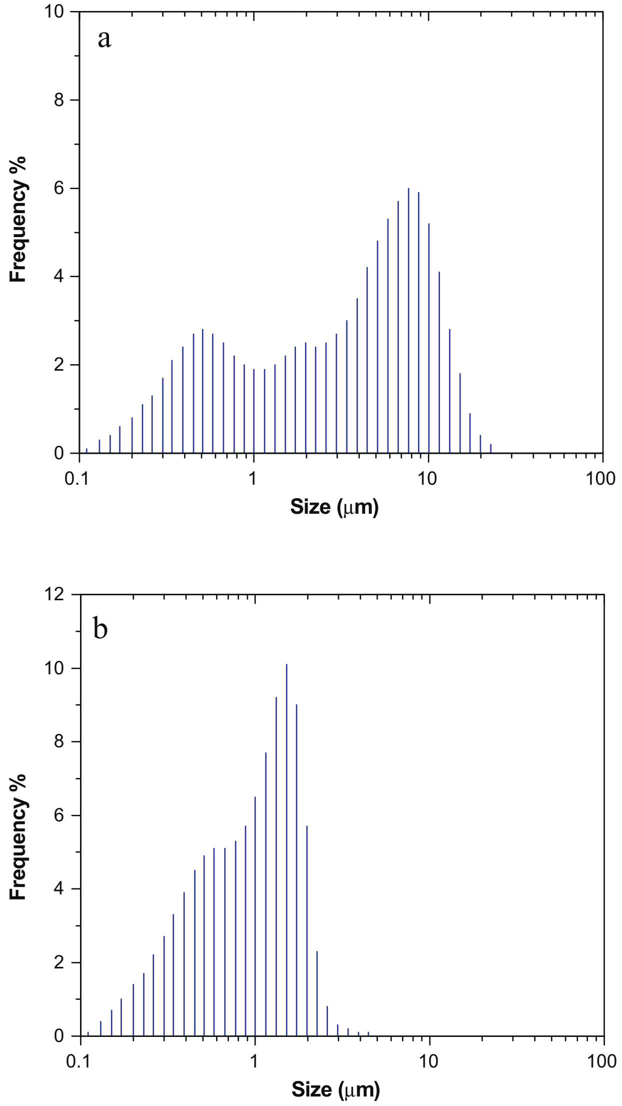

Fig. 5. Particle size distributions of $GdAlO_3$ powders produced through combustion reaction of gadolinium–aluminium nitrates (a) with urea and β-alanine; (b) with urea and glycine.

in color indicating the presence of residual carbon. The amorphous nature of the resulting powders was also confirmed by XRD. On the other hand, $Gd(NO_3)_3$–glycine mixture when heated on hot plate, resulted in flame combustion. The powder obtained after combustion process was white in color. The XRD pattern of the powder is shown in Fig. 2(a). The pattern exhibits all the reflection corresponding to monoclinic polymorph of Gd_2O_3 phase [ICDD PDF 012-0474]. The average crystallite size of the powder calculated from X-ray line broadening is 20.4 nm. In the case of $Gd(NO_3)_3$–β-alanine mixture, heating of the solution resulted in relatively violent combustion process which yielded white colored powder. The XRD pattern of the powder, as shown in Fig. 2(b), confirms that the powder is phase pure m-Gd_2O_3. The average crystallites size of Gd_2O_3 obtained is 42.2 nm. This value is higher than the average crystallites size of m-Gd_2O_3 obtained by using glycine as fuel, which suggests that the combustion temperature was higher when β-alanine was employed.

Based on the above results, it can be inferred that the combustion characteristics of $Gd(NO_3)_3$, and $Al(NO_3)_3$ towards a specific fuel is different. Unlike $Al(NO_3)_3$, urea is not an appropriate fuel for $Gd(NO_3)_3$ for combustion reaction to yield the desired crystalline oxide phase. For $Gd(NO_3)_3$, glycine and β-alanine are suitable fuels that yield the desired oxide phase after the combustion reaction.

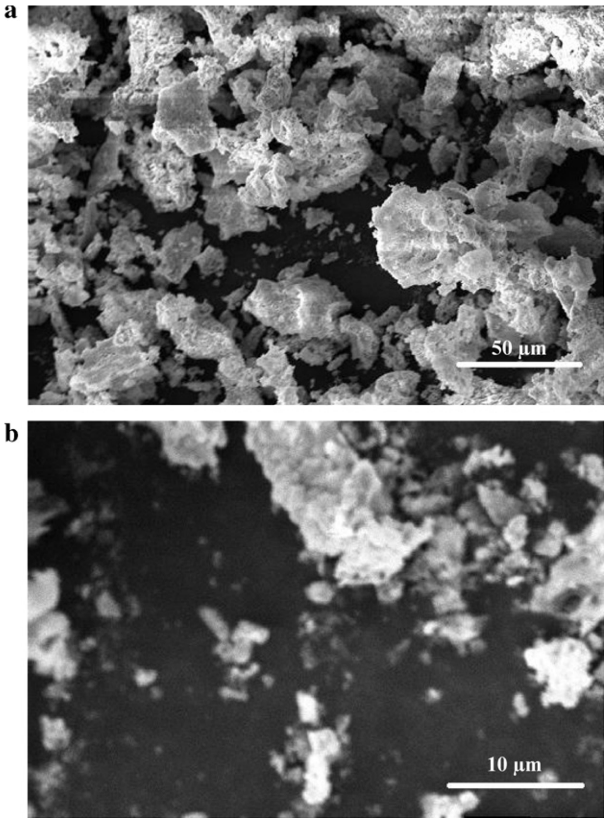

Fig. 6. SEM photomicrographs of $GdAlO_3$ powders produced through combustion reaction of gadolinium–aluminium nitrates (a) with urea and β-alanine; (b) with urea and glycine.

Considering that urea is the suitable fuel for $Al(NO_3)_3$, one may conclude that in the case of a stoichiometric mixture containing $Gd(NO_3)_3$, $Al(NO_3)_3$ and urea, for preparation of $GdAlO_3$ powder, $Gd(NO_3)_3$ may act as an inhibitor, reducing the intensity of the combustion reaction between $Al(NO_3)_3$ and urea and thereby reducing the temperature within the reaction mixture. Experimentally, it has found to be true, as for sample GA-U (Table 1), dehydration of nitrates–urea mixture did not result in any combustion reaction that yielded a white powder. The amorphous nature of the powder was confirmed by XRD.

The reactions of mixtures containing $Gd(NO_3)_3$ and $Al(NO_3)_3$ with glycine (sample GA-G) or β-alanine (sample GA-B) result in weak smouldering combustion reaction. It may be mentioned that glycine and β-alanine are the fuels that react very aggressively with $Gd(NO_3)_3$ and considerably less energetically with $Al(NO_3)_3$. The resulted powders for GA-G and GA-B samples exhibited a brown color indicating the presence of residual carbonaceous material. This suggests that the temperature within the reactant system was not very high, which is reflected by the amorphous nature of these powders as confirmed by XRD.

3.1.2. *Use of fuel mixture*

Taking into consideration of the amorphous character of the powders obtained by using a single fuel, one can conclude that the metal nitrate-fuel combinations used in samples 7–9 cannot produce $GdAlO_3$ phase without a subsequent calcination step. The use of two-fuel mixtures – selected according to the combustion characteristics of metal nitrate with respect to the three fuels – has major consequences on the combustion mode

Table 2

Lattice parameters and cell volume of $GdAlO_3$ phase obtained after Rietveld refinement of XRD data along with similar data from standard pattern of the phase for comparison.

Lattice Parameters (Å)/Cell Volume (Å^3)	$GdAlO_3$ GA-UB*	$GdAlO_3$ GA-UG**	$GdAlO_3$ ICDD PDF 046-0395	$GdAlO_3$ Single crystal [23]
a	5.2999(4)	5.2999(5)	5.3017(2)	5.3049(7)
b	7.4430(4)	7.4430(7)	7.4450(3)	7.4485(9)
c	5.2533(3)	5.2535(4)	5.2511(3)	5.2537(6)
Cell Vol.	207.23(2)	207.24(3)	207.27	207.59(4)

Reliability factors for refinement: *GA-UB: Rp: 4.79%; Rwp: 6.08%; Rexp: 5.36%; χ^2: 1.29. **GA-UG: Rp: 5.23%; Rwp: 6.72%; Rexp: 6.07%; χ^2: 1.23.

and characteristics of the final powder. In the sample 10 (GA-UG), containing $Al(NO_3)_3$, $Gd(NO_3)_3$ and a mixture of urea and glycine (urea: the appropriate fuel for $Al(NO_3)_3$ and glycine – one of the suitable fuels for $Gd(NO_3)_3$), the combustion reaction was found to propagate uniformly throughout the reaction vessel resulting in a voluminous white colored powder. Similar reaction took place between $Al(NO_3)_3 + Gd(NO_3)_3$ and a mixture of urea and β-alanine (Sample 11: GA-UB) yielding a voluminous white powder. Figs. 3 and 4 show the Rietveld analysis patterns of as synthesised GA-UB and GA-UG powders respectively. All the reflections of both the powders correspond to perovskite $GdAlO_3$ phase [ICDD PDF 046-0395]. The tick marks below the patterns represent the positions of all possible Bragg reflections. The lower solid line represents the difference between the observed and calculated intensities. In general, the Rietveld method utilises the least-squares refinement for obtaining the best fit between the experimental data and the calculated pattern based on the simultaneously refined models. In the present investigation, a Thomson-Cox-Hasting pseudo-Voigt peak profile function [20] was used for the profile fitting. The analysis was accomplished assuming PNMA space group for orthorhombic distorted perovskite structure. The background was taken to be the polynomial function of 2θ of the sixth order as it facilitated the best fit.

Refined lattice parameters of $GdAlO_3$ phase obtained through Rietveld refinement are given in Table 2. The quality of the agreement between observed and calculated profiles is evaluated by profile factor (R_p), weighted profile factor (R_{wp}), expected weighted profile factor (R_{exp}), and reduced chi-square (χ^2). The mathematical expressions of the above parameters can be found elsewhere [21]. The values of the reliability parameters vet the refinements. The lattice parameters obtained after Rietveld refinements are in good agreement with the reported values of the orthorhombic crystal structure of $GdAlO_3$ phase [ICDD PDF 046-0395].

In the field of combustion synthesis, there has been a trend to calculate the adiabatic flame temperature of combustion reaction in order to co-relate the crystallite size of the product with the process parameters. However, many a times, it has been observed that the calculated adiabatic flame temperature is far from the actual temperature of the flame. This is due to loss of heat via different transfer mode to the surroundings as well as the occurrence of controlled combustion in a time scale where adiabatic condition does not hold good. Hence, in the present investigation, the actual flame temperature was measured using an optical pyrometer. The flame temperature of combustion reaction between Gd-Al nitrates and urea + glycine was found to be $890 \pm 10\,^\circ C$, while the same for combustion reaction between nitrates and urea + β-alanine was $1035 \pm 10\,^\circ C$.

From the X-ray line broadening it was observed that $GdAlO_3$ powders were nanocrystalline; the calculated crystallite sizes of GA-UG and GA-UB powders were 37 and 57 nm respectively. The larger crystallite size of GA-UB powder as compared to that of GA-UG powder can be attributed to the higher flame temperature of the combustion reaction.

3.2. Characterization of powder particles

The particle size distributions of $GdAlO_3$ powders prepared through combustion reaction using urea- β-alanine and urea–glycine fuel mixtures are shown in Fig. 5(a) and (b). The $GdAlO_3$ powder prepared using urea–glycine fuel mixture shows monomodal particle distribution with median particle size of 0.91 μm. However, for $GdAlO_3$ powder prepared using urea–β-alanine fuel mixture, a bimodal particle distribution was observed with modes at 0.51 μm and 7.7 μm respectively. The SEM photomicrographs of as synthesized GA-UB and GA-UG powders are shown in Fig. 6(a) and (b) respectively. The morphologies of powders suggest that they are composed of porous, soft agglomerates containing nanocrystalline grains. The large amount of gases generated during combustion synthesis facilitates rapid cooling leading to nucleation of crystallites without any substantial growth. The gas generated also helps to disintegrate the large particles or agglomerates; therefore, the resulted product consists of very fine particles of friable agglomerates or nanoparticles.

3.3. Sintering study

One of the possible demerits of combustion synthesis process could be the formation of hard agglomerates in the powder if the flame temperature is not controlled. This can lead to lowering of density in the sintered mass. In order to confirm the sinterability of the powders produced through these routes, powders GA-UB and GA-UG were sintered in the temperature range of 1400–1550 °C for 4 h. Fig. 7(a)–(d) show the SEM photomicrographs of as sintered specimens of $GdAlO_3$ produced from GA-UB powder and sintered at different temperatures. At 1400 °C, the first stage of sintering takes place which is reflected by neck formation. The powder particles tend to loose their identities at 1450 °C where neck growth takes place indicating the presence of interconnected porosity. The density of the specimen at this temperature was 90% of the theoretical value. At 1500 °C, the powder sinters to specimen having density more than 95% T.D. The micrographs of $GdAlO_3$ from GA-UB (Fig. 7(c) and (d)) exhibit dense microstructure with uniform grain structure, with an average grain size of 15 μm. There was no second phase present in the microstructure that confirms the phase purity of $GdAlO_3$ that was earlier indicated by XRD results.

Fig. 8(c) and (d) show the SEM photomicrographs of as sintered specimens of $GdAlO_3$ produced from GA-UG powder and sintered at different temperatures. It can be observed from the micrographs that the onset of sintering takes place at a higher temperature in the GA-UG powder as compared to that of GA-UB powder. At 1450 °C, the neck formation starts indicating the occurrence of first stage of sintering. At 1500 °C, the powder sinters to specimen having density of 88% T.D, which is less than the density of sintered specimen derived from GA-UB powder. The micrograph of GA-UG specimen sintered at 1550 °C, as shown in Fig. 8(d), exhibits dense microstructure (with >95% T.D. density) with uniform grain structure, with an average grain size of 5 μm.

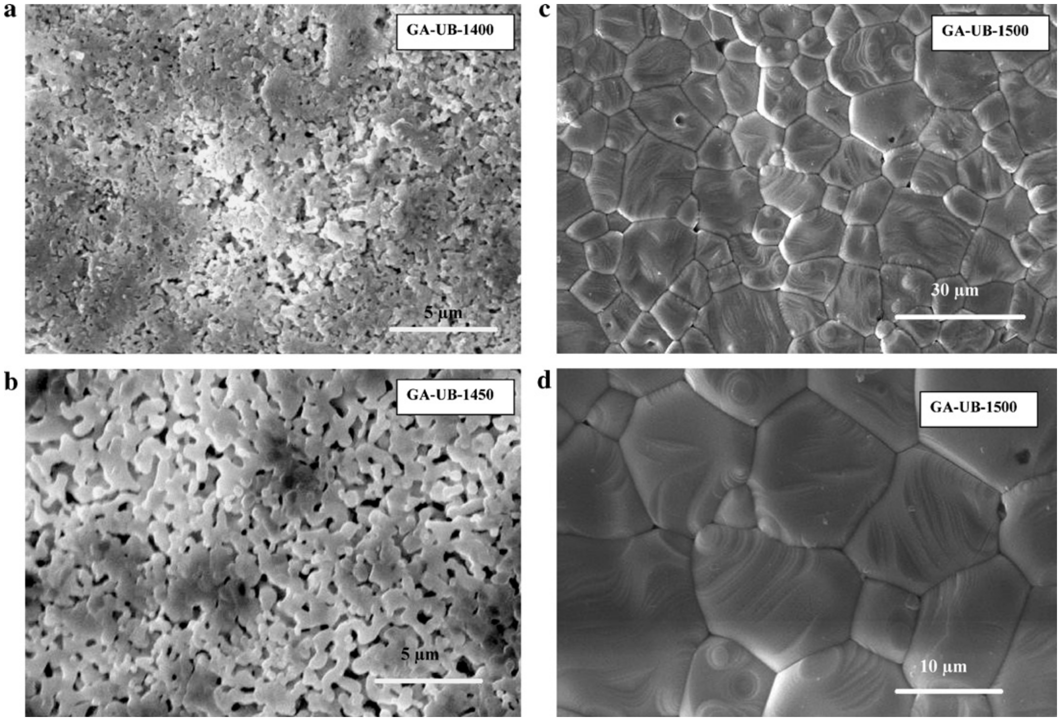

Fig. 7. SEM photomicrographs of as sintered specimens of $GdAlO_3$ derived from powder produced through combustion reaction of gadolinium–aluminium nitrates with urea and β-alanine which are sintered at (a) 1400 °C; (b) 1450 °C; (c) and (d) 1500 °C respectively for 4 h.

From the sintering study, it was observed that GA-UB powder could be densified at 1500 °C while the powder GA-UG requires a slight higher temperature of 1550 °C. It may be mentioned here that the sintering of $GdAlO_3$ powder produced through solid state synthesis route requires a sintering temperature of 1700 °C to achieve a sintered density of more than 95%. T.D. [22]. The sintering temperature of GA-UB powder is thus 200 °C lower than that for $GdAlO_3$ powder produced through conventional solid state synthesis route. The grain size in the final microstructure of GA-UG is finer than that for GA-UB indicating grain growth phenomena taking place in powder GA-UB while sintering at 1500 °C. The present study shows that the direct formation of $GdAlO_3$ powder using the fuel mixture does not adversely affect the sinterability of the powder. The powders produced in the present

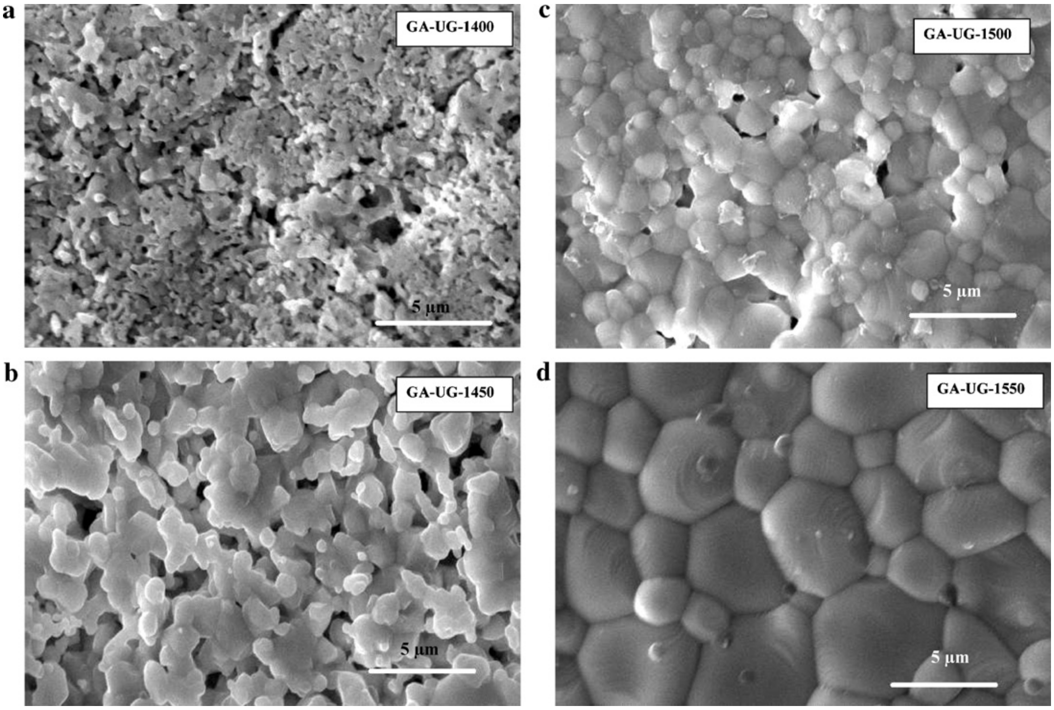

Fig. 8. SEM photomicrographs of as sintered specimens of $GdAlO_3$ powder produced through combustion reaction of gadolinium–aluminium nitrates with urea and glycine which are sintered at (a) 1400 °C; (b) 1450 °C; (c) 1500 °C and (d) 1550 °C respectively for 4 h.

investigation are highly sinterable without any further grinding.

4. Conclusions

In the present investigation, it has been observed that gadolinium and aluminium nitrates offer different combustion characteristics with respect to different fuels for the formation of respective oxides. Among the three fuel studied, for aluminium, urea was found to be best fuel for preparation of α-Al_2O_3 directly after combustion reaction. For gadolinium, glycine and β-alanine are better fuels for direct phase formation. For the preparation of $GdAlO_3$ powder, the use of a single fuel, as it is usually done in traditional combustion synthesis, leads to the formation of an amorphous precursor powder. The use of fuel mixtures (urea and β-alanine or urea and glycine) facilitates direct formation of phase pure, nanocrystalline $GdAlO_3$, in a single step. The process essentially ensures a significant reduction in energy consumption as well as the possibility of mass scale production of nano-crystalline $GdAlO_3$ powder. The powders produced through these routes could be sintered to dense bodies having a sintered density of more than 95% T.D. after sintering at 1550 °C.

References

[1] S.D. Han, S.P. Khatkar, V.B. Taxak, D. Kumar, J.Y. Park, Mater. Sci. Eng. B 127 (2–3) (2006) 272–275.
[2] G.S.R. Raju, J.Y. Park, H.C. Jung, B.K. Moon, J.H. Jeong, J.H. Kim, Curr. Appl. Phys. 9 (1) (2009) e92–e95.
[3] S.A. Smirnovaa, Li. Kazakova, A.A. Fyodorovh, M.V. Korzhik, J. Lumin. 60–6l (1994) 960–962.
[4] J.W.M. Verweij, M.Th. Cohen-Adad, D. Bouttet, H. Lautesse, B. Moine, C. Pédrini, Chem. Phy. Lett. 239 (1995) 51–55.
[5] A. Sinha, B.P. Sharma, P. Gopalan, Electrochim. Acta 51 (2006) 1184–1193.
[6] A. Sinha, H. Näfe, B.P. Sharma, P. Gopalan, J. Electrochem. Soc. 155 (3) (2008) B309–B314.
[7] G. Cao, Nanostructures and Nanomaterials. Synthesis, Properties and Applications, Imperial College Press, London, 2004.
[8] H.H.S. Oliveira, M.A. Cebim, A.A. Da Silva, M.R. Davolos, J. Alloys Compd. 488 (2009) 619–623.
[9] H. Gao, Y. Wang, J. Lumin. 122–123 (2007) 997–999.
[10] S. Cizauskaite, V. Reichlova, G. Nenartaviciene, A. Beganskiene, J. Pinkas, A. Kareiva, Mater. Chem. Phys. 102 (1) (2007) 105–110.
[11] A. Sinha, B.P. Sharma, H. Näfe, P. Gopalan, J. Alloys Compd. 502 (2010) 396–400.
[12] R.M. Trommer, A.K. Alves, C.P. Bergmann, J. Alloys Compd. 491 (2010) 296–300.
[13] T.-W. Chiu, B.-S. Yu, Y.-R. Wang, K.-T. Chen, Y.-T. Lin, J. Alloys Compd. (2010), doi:10.1016/j.jallcom.2010.11.162.
[14] A. Ainirad, M.M. Kashani Motlagh, A. Maghsoudipoor, J. Alloys Compd. (2010), doi:10.1016/j.jallcom.2010.10.137.
[15] N. Chaiyo, R. Muanghlua, S. Niemcharoen, B. Boonchom, N. Vittayakorn, J. Alloys Compd. (2010), doi:10.1016/j.jallcom.2010.11.043.
[16] S.R. Jain, K.C. Adiga, V.R. Pai Venekar, Combust. Flame 40 (1981) 71–79.
[17] A.L. Patterson, Phy. Rev. 56 (1939) 978–982.
[18] T. Roisnel, J. Rodríguez-Carvajal, in: R. Delhez, E.J. Mittemeijer (Eds.), Proceedings of the Seventh European Powder Diffraction Conference (EPDIC 7), 2000, p. 118.
[19] M. Mendelson, J. Am. Ceram. Soc. 52 (1969) 443–446.
[20] P. Thompson, D. Cox, J. Hastings, J. Appl. Cryst. 20 (1987) 79–83.
[21] H.M. Rietveld, J. Appl. Cryst. 2 (1969) 65–71. Fullprof. Suite program available at http://www.llb.cea.fr/fullweb/fp2k/fp2k.htm.
[22] A. Sinha, PhD Thesis, Indian Institute of Technology, Bombay, Mumbai, India, 2008.
[23] D.D. Boulay, N. Ishizawa, E.N. Maslen, Acta Cryst. C60 (2004) i120–122.